堆焊快速成形低碳钢件的裂纹形成机理

李 超, 梁媛媛, 沈灿铎, 朱 胜
(装甲兵工程学院 装备再制造技术国防科技重点实验室, 北京 100072)

摘 要: 采用 SEM观察了堆焊快速成形低碳钢件的裂纹微观形貌. 结果表明, 裂纹萌生于成形件的初始沉积层, 沿沉积高度方向扩展, 终止于成形件表面之下. 采用 OM和 EDS分析了成形件中的偏析与夹杂物成分, 利用 XRD分析了成形件中的残余奥氏体含量, 成形件中的裂纹为液化热裂纹, 在多层多道连续堆焊成形过程中, Mn Si的氧化物、Mo的碳化物以及 N金属间化合物的偏析是裂纹形成的内因, 拉应力是裂纹形成的外因. 通过合理匹配 Mn Ni Si元素的含量, 添加稀土元素 Ce净化焊缝金属, 采用层层正交的路径沉积, 延长层间隔时间, 可以消除堆焊快速成形低碳钢件的裂纹.

关键词: 堆焊; 快速成形; 金属芯焊丝; 裂纹; 偏析
中图分类号: TG142 文献标识码: A 文章编号: 0253-360X(2010)09-0053-04

李 超

0 序 言

焊接快速成形技术是基于离散/堆积的原理, 通过三维实体扫描或直接建模获得三维实体模型, 将模型沿某一坐标方向按一定的厚度进行分层切片处理, 然后由焊接热源将金属丝材(粉末)熔化, 按设定的成形路径堆积成形每一薄层, 由层层堆积最终形成全焊缝金属零件的先进制造技术. 可见, 焊接快速成形技术是一种典型的分层制造技术. 焊接快速成形技术具有制造成本低、生产效率高、制造形式灵活、成形件性能好等优点[1,2]. 按照快速成形所采用的焊接工艺分类, 焊接快速成形技术可分为熔化极气体保护焊、钨极气体保护焊、微弧等离子焊、激光束焊、电子束焊等. 其中, 基于熔化极气体保护焊的堆焊快速成形技术在大尺寸金属零件的快速制造/再制造成形方面具有显著的优势.

堆焊快速成形过程中, 若成形材料、工艺参数或者路径规划的选择不当, 可能导致成形件产生裂纹. 裂纹一旦产生, 将沿着沉积层不断扩展, 严重影响成形件的性能, 导致成形件报废[3,4]. 可见, 对堆焊快速成形过程中裂纹形成机理的研究具有重要意义. 为此, 采用微观测试分析的方法, 深入研究了以 Fe-Mn-Si-Ni-Mo系微渣型金属芯焊丝作为成形材料时成形件的裂纹形成机理, 并提出了减少或消除成形件裂纹的方法, 为消除堆焊快速成形过程中成形件的裂纹产生提供理论依据.

收稿日期: 2009-04-20
基金项目: 国家自然科学基金资助项目(50975286); 中国机械工程学会焊接学会创新思路预研奖学金资助项目

1 试验方法

采用装备再制造技术国防科技重点实验室开发的"基于机器人的 MIG/MAG堆焊熔敷快速成形系统", 该系统集成了可离线编程控制的 ABB机器人和 Fronius TPS4000型 MIG/MAG焊接系统. 焊接工艺参数为送丝速度 5.0 m/min, 电弧电压 23.2~24.3 V, 焊接电流 130~140 A, 焊接速度 10 mm/s, 焊丝伸出长度 10~15 mm, 保护气体 80% Ar+20% CO_2, 气体流量 18~20 L/min. 基板采用 200 mm×100 mm×8 mm的 Q235钢. 堆焊成形材料为自制的金属芯焊丝, 直径 1.2 mm, 熔敷金属主要成分(质量分数, %)为 C 0.08, Si 0.33, Mn 2.57, Mo 0.44, Ni 2.33, Fe余量.

按照"弓"字形轨迹逐层进行扫描, 连续堆焊 8层, 制备的成形件尺寸为 120 mm×60 mm×15 mm. 采用电火花线切割将成形件的 A截面切开, A截面的宏观裂纹如图 1所示, 然后将试样磨平、抛光, 经 5%硝酸酒精溶液刻蚀后, 采用 Olympus PMG-3型金相显微镜和 Quanta 200型环境真空扫描电镜观察试样裂纹的微观形貌; 采用 EDAX Genesis型能谱仪分析试样中的偏析和夹杂物的成分; 采用 D8 ADVANCE型 X射线衍射仪分析成形件中的残余奥氏体的含量.

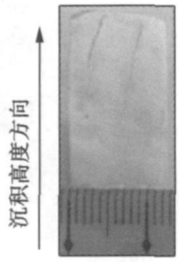

图 1 裂纹的宏观形貌

Fig. 1 Macroscopic morphology of cracks

2 裂纹形成机理分析

采用扫描电镜观察图 1所示的裂纹微观形貌如图 2所示. 结合图 1可见, 裂纹萌生于成形件的初始沉积层, 沿沉积高度方向不断扩展, 终止于成形件表面之下, 表面无裂纹出现.

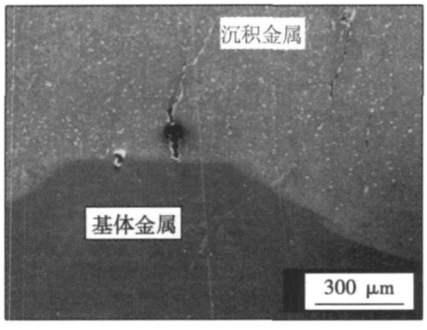

(a) 裂纹形成区域

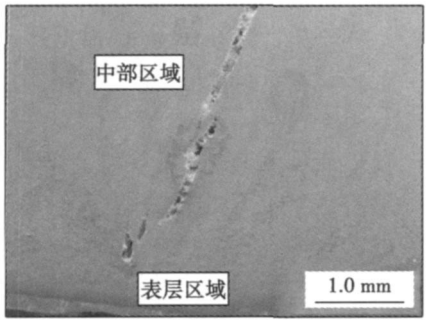

(b) 裂纹终止区域

图 2 裂纹的微观形貌

Fig. 2 Micromorphology of cracks

图 3表明了裂纹形成与偏析、夹杂物的关系. 由图 3可见, 偏析是裂纹形成的前因, 裂缝形成后, 部分偏析成分形成夹杂物并聚集于裂缝之中. 在裂缝扩展受阻改变方向后, 裂纹沿产生偏析的方向萌生; 在裂缝中, 偏析成分形成球形夹杂物进入缝隙. 在尚未形成裂缝的区域, 偏析聚集形成带状. 裂缝中间含有球形和具有光滑表面的夹杂物, 说明该裂纹是由于偏析成分在高温下形成液膜, 冷却过程中液膜与两侧晶粒分离而导致的液化热裂纹.

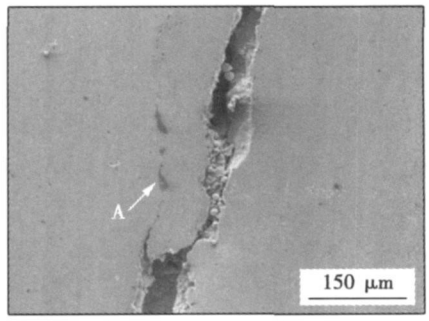

图 3 裂纹与偏析、夹杂物的关系

Fig. 3 Location of cracks and segregation & inclusion

成形件的主要组织是块状和条状先共析铁素体、针状铁素体、少量的珠光体和残余奥氏体. 由于堆焊成形过程中相邻焊道的热影响作用, 成形件的组织在局部范围内呈现一定的方向性, 如图 4所示. 由图 4可见, 成形件中的裂纹主要存在于不同生长方向的晶界之间, 沿晶界曲线延伸, 遇到尺寸较大、生长方向一致的组织时发生偏转分叉, 随着促进裂纹形成的能量不断耗散, 裂纹最后终止.

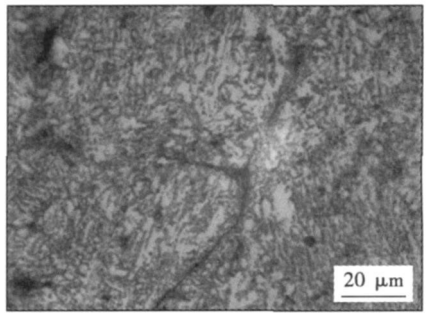

图 4 裂纹与偏析

Fig. 4 Cracks and segregation

对图 3中偏析带上的 A点进行 EDS分析, 如图 5所示. 由图 5可见, C、O、Mn、Si、Mo和 N元素的含量均显著高于成形件的化学成分含量. 因此, 偏析的主要成分应是 Mn和 S的氧化物、Mo的碳化物以及 N的金属间化合物. Mn和 S的氧化物在一定条件下会形成低熔点的锰硅酸盐, 其熔点可低至 1 200 ℃左右[5]. 在多层多道焊的热循环过程中, 如果部分锰硅酸盐来不及上浮到沉积层表面, 残留在沉积层内部的锰硅酸盐在晶界上富集, 形成低熔点的液态薄膜, 最终在拉伸应力作用下导致结晶裂纹.

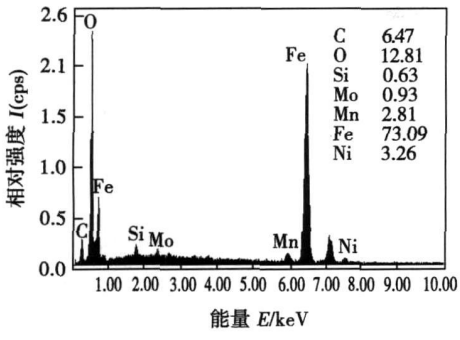

图 5　图 3中 A点的 EDS分析

Fig. 5　EDS of spot A in Fig. 3

对成形件中的 α和 γ相含量分析表明，成形件的残余奥氏体平均含量为 10.55%．奥氏体可以显著降低有害元素 S，P的溶解度，造成有害元素的偏析．同时，Mo元素在奥氏体中的体扩散系数较小，又是强碳化物形成元素，其碳化物在奥氏体枝晶生长过程中容易偏析，使碳化物大量弥散分布于奥氏体枝晶间，造成材料基体组织和晶界间的浓度差别，产生晶界脆化，在拉应力作用下引起沿晶裂纹[6]．残余奥氏体的存在还导致成形件的导热系数低于低碳钢基板的导热系数，而线膨胀系数大于低碳钢基板的线膨胀系数．因此，在多层多道堆焊过程中容易在焊缝金属中形成较大的拉伸应力，使得成形件的热裂敏感性显著增加．

综合以上分析，成形件中的裂纹形成机理为多层多道堆焊成形过程中，由于相邻焊道或下一沉积层对上一沉积层的热影响作用，偏析聚集在奥氏体晶界处的低熔点锰硅酸盐发生重熔，碳化物引起材料基体组织和晶界间产生浓度差，使焊缝金属产生脆性温度区，在拉伸应力的作用下，沿原奥氏体晶界开裂形成液化裂纹．液化裂纹一旦形成，在拉应力的持续作用下，沿着沉积层之间的晶界向下一层不断扩展，形成宏观裂纹．

3　影响裂纹形成的因素

3.1　合金成分

堆焊成形材料合金体系的设计不仅要考虑单个元素对焊缝金属强韧性的作用，还要考虑与其它元素的协同作用．从提高成形件强度和韧性的角度出发，提高了成形材料中 Mn和 N元素的含量．事实表明，只有 Mn，N，i S元素在最佳含量范围内才能有效地提高成形件的强韧性，并防止成形件产生热裂纹缺陷．图 6所示为 Mn，N元素含量对焊缝金属形成热裂纹的影响[5]，图 6中 A_{KV}为 −20 ℃条件下 V形缺口试样的冲击吸收功，σ_y为 y方向正应力．由图 6可见，Mn，N元素的含量过高时，将会导致焊缝金属热裂纹的形成．

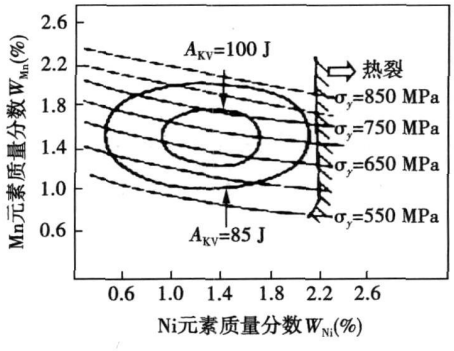

图 6　Mn和 N元素含量对焊缝金属热裂纹的影响

Fig. 6　Effects of Mn and Ni on hot cracks

3.2　夹杂物

对裂纹中的夹杂物进行能谱分析，结果如表 1所示．可见，夹杂物与偏析的主要成分基本一致，一方面验证了裂纹中夹杂物来源于偏析的推论，另一方面也说明了裂纹的形成与 Mn和 S的氧化物、Mo的碳化物以及 N的金属间化合物有关．

表 1　夹杂物的能谱分析（质量分数，%）

Table 1　EDS of inclusions

夹杂	C	O	Si	Mn	Mo	Ni	Fe
1	2.36	0.81	0.30	—	0.62	2.55	93.36
2	2.34	1.50	0.49	1.90	0.68	2.54	90.54
3	2.08	0.60	0.40	—	3.65	—	93.27
4	1.26	0.51	0.42	2.28	1.14	2.74	91.66

3.3　应力分布

在堆焊快速成形过程中，焊缝金属会经历剧烈的温度变化．当熔池金属凝固收缩时，由于受到周围凝固金属和基板的限制，不能自由收缩，导致焊缝金属中产生拉伸应力．通过 ANSYS软件模拟单层沉积层中心点的应力—时间变化结果表明[7]，沉积层中焊缝金属承受的最大拉伸应力超过 250 MPa，这个拉伸应力远大于存在残余液相的凝固金属的塑性和强度极限，直接导致凝固金属组织沿晶开裂，并且持续作用的拉应力促使裂纹沿沉积方向不断扩展．因此，焊缝金属中的拉伸应力是形成裂纹的主要外因．

4　减少裂纹形成的措施

基于上述裂纹形成影响因素的分析，可以从三

个方面采取措施来减少或消除成形件中的裂纹. (1)适当降低奥氏体化元素(如 Mn, Ni元素)的含量,合理匹配 Mn, Ni, S元素的含量,避免这些元素带来的不利影响. (2)通过添加稀土元素 Ce,净化焊缝金属,使偏析球化,避免奥氏体晶界处形成液化薄膜. (3)采用层层正交的路径沉积,延长层间隔时间,降低层间隔温度,减少焊缝金属凝固过程中的应力累积,防止焊缝金属产生拉应力集中. 通过以上改进,对堆焊成形低碳钢件进行分析,均无裂纹产生.

5 结 论

堆焊成形件的裂纹萌生于初始沉积层,沿沉积高度方向扩展,终止于成形件表面之下,属沿晶液化热裂纹. 在多层多道堆焊成形过程中,Mn和 S的氧化物、Mo的碳化物以及含 N金属间化合物的偏析是裂纹形成的内因,焊缝金属凝固产生的拉应力是裂纹形成的外因. 通过合理匹配 Mn, Ni, S元素的含量,添加稀土元素 Ce改进成形材料,采用层层正交的路径沉积,延长层间隔时间,可以消除成形件的裂纹.

参考文献:

[1] 李 超,朱 胜,沈灿铎,等. 焊接快速成形技术的研究现状与发展趋势[J]. 中国表面工程, 2009, 22(3): 7-12.
Li Chao, Zhu Sheng, Shen Canduo, et al. Present state and development trend of welding rapid forming technology[J]. China Surface Engineering, 2009, 22(3): 7-12.

[2] Zhang Yuming, Li Pengjiu, Chen Yiwei, et al. Automated system for welding-based rapid prototyping[J]. Mechatronics, 2002, 12: 37-53.

[3] 陈 静,林 鑫,王 涛,等. 316L不锈钢激光快速成形过程中熔覆层的热裂机理[J]. 稀有金属材料与工程, 2003, 32(3): 183-186.
Chen Jing, Lin Xin, Wang Tao, et al. The hot cracking mechanism of 316L stainless steel cladding in rapid laser forming process[J]. Rare Metal Materials and Engineering, 2003, 32(3): 183-186.

[4] 赵晓明,陈 静,何 飞,等. 激光快速成形 Rene88DT高温合金开裂机理研究[J]. 稀有金属材料与工程, 2007, 36(2): 216-220.
Zhao Xiaoming, Chen Jing, He Fei, et al. The cracking mechanism of rene88DT superalloy by laser rapid forming[J]. Rare Metal Materials and Engineering, 2007, 36(2): 216-220.

[5] 陈伯蠡. 焊接冶金原理[M]. 北京: 清华大学出版社, 1991.

[6] 钟定铭,刘建国,银锐明,等. 堆焊金属裂纹形成机理研究[J]. 株洲工学院学报, 2002, 16(6): 87-89.
Zhong Dingming, Liu Jianguo, Yin Ruiming, et al. Study on the principle of formation of heap soldering metal cracks[J]. Journal of Zhuzhou Institute of Technology, 2002, 16(6): 87-89.

[7] 赵继勋. 基于机器人 GMAW堆焊再制造成形层数值模拟研究[D]. 北京: 装甲兵工程学院, 2008.

作者简介: 李 超,男,1979年出生,博士研究生. 主要从事焊接快速成形技术方面的研究. 发表论文 8篇.
Email: lichaomse@yahoo.cn

tents of alloying elements in the grain boundary were less than those in the base material and heat-affected zone. The crystal cracks for welding in ZM6 magnesium alloy casting were found by observing the crack location and investigating the process of welding of ZM6 magnesium alloy casting.

Key words: ZM6 magnesium alloy casting; TIG repairing welding; process method

Effect of pulse current frequency on microstructure and mechanical properties of 2219 aluminum alloy weld joints

CONG Baoqiang, QI Bojin, LI Wei, YANG Mingxuan (School of Mechanical Engineering and Automation, Beihang University, Beijing 100191, China). p. 37—40

Abstract: The influence of pulse square-wave current frequency on the microstructure and mechanical properties of 2219 high strength aluminum alloy weld joints was investigated based on a novel ultrafast-convert hybrid pulse current variable polarity gas tungsten arc welding technique. The experimental results showed that comparing with no effect of pulse current, the coarse grains changed to fine equiaxed grains. A kind of finer equiaxed non-dentrites was observed distributing in the form of banding at the weld zone while the pulse current frequency was more than 20 kHz. Mechanical properties of weld joints were improved predominantly at the given pulse frequency of 60 kHz, tensile strength and percentage elongation of weld joints are increased by about 17.6% and 66%, respectively, compared to that of weld joints with no effect of pulse current. At the given pulse current amplitude and pulse duty cycle, with the pulse current frequency in certain range increased, the width of fusion zone obviously decreased and the ductility of welds was improved significantly. However, the variation in tensile strength of weld joints was relatively less sensitive with the increase of pulse current frequency.

Key words: high strength aluminum alloy; high frequency pulse current; pulse frequency; equiaxed non-dentrite; mechanical property

Formation characteristics of Ni/Ti intermetallics through annealing of layered Ni/Ti

ZHOU Yong-2, YANG Guan-Jun1, WU Xian2, LI Changjiu1 (1. State Key Laboratory for Mechanical Behavior of Materials, School of Materials Science and Engineering, Xi'an Jiaotong University, Xi'an 710049, China; 2. School of Materials Science and Engineering, Xi'an Shiyou University, Xi'an 710065, China). p. 41—44

Abstract: Ni/Ti diffusion couples were prepared by cold spraying with Ni and Ti powders and mechanically alloyed Ni/Ti alloy powders. The formation and growth characteristics of Ni/Ti intermetallics within Ni/Ti during solid state diffusion treatment were investigated by scanning electron microscopy (SEM) and X-ray diffraction (XRD). It was found that the thicknesses of Ni_3Ti, NiTi and Ti_2Ni intermetallic compounds layers increased with annealing temperature. The growth of TiNi layer followed the parabolic law with annealing time while the thicknesses of Ti_2Ni or Ni_3Ti layers were kept constant at certain annealing temperature. The results suggest that the formation and then rapid growth of TiNi intermetallic take place after Ni_3Ti and Ti_2Ni intermetallic compounds grow to certain thicknesses.

Key words: Ni/Ti diffusion couples; solid state diffusion; annealing treatment; intermetallic compound

Study of digital push-pull CO_2 welding system

LU Zhenyang, YAN Sibo, YANG Shuai, LIU Jia (College of Mechanical Engineering & Applied Electrons Technology, Beijing University of Technology, Beijing 100124, China). p. 45—48, 52

Abstract: The digital Push & Pull CO_2 welding system is proposed. This system utilize digital power source controlled by DSP and CPLD as platform with the AC servo push-pull feeder with the low moment of inertia, fast response, and steady feed speed. The constant feeding part combine with push-pull feeding part to form the whole feeder using buffer as a linker. Consider the characteristics of the push-pull short-circuit CO_2 welding technics, the feeder speed curve, welding voltage and current waveform control program was pre-designed. According to software program, the steady push-pull CO_2 welding technics was achieved with low spatter, low heat input and uniform droplet.

Key words: digital power source; push-pull feeder; CO_2 welding; low heat input

Study on structures and properties of part made by micro-plasma arc direct metal formation

XIANG Yonghua-2, XU Binshi1, LV Yaohui1 (1. Navy Logistic Technology and Equipment Institute of PLA, Beijing 100072, China; 2. National Key Laboratory for Remanufacturing, Academy of Armored Forces Engineering, Beijing 100072, China). p. 49—52

Abstract: The deposition experiments were done on the mild steel by micro-plasma arc powder overlaying rapid prototyping technique with Fe313 alloy powder. The microstructures and morphologies were observed by metallographic microscope and SEM, the microhardness was tested by vickers. It was showed that the middle layer displayed insular M-A component structure, and the interface between layers was evident. The microstructure of Fe-based deposited layer was affected by the subsequent overlaying with annealing process, and the crystalline grain refined. The hardness distribution curve of the cylindraceous part was as U shape, the middle layer was soften because the drawing effect of subsequent layers.

Key words: rapid prototyping; micro-plasma arc overlaying; Fe-based alloy; microstructure

Cracking formation mechanism of mild steel parts fabricated by surfacing rapid forming

LI Chao, LIANG Yuanyuan, SHEN Canduo, ZHU Sheng (National Defence Key Laboratory for Remanufacturing, Academy of Armored Forces Engineering, Beijing 100072, China). p. 53—56

Abstract: The micro-morphology of cracks for the parts fabricated by surfacing rapid forming was observed with SEM. The results showed that the cracks initiated from the first layer of the part, extended along the deposition direction, and finally terminated under the surface of the part. The segregation and inclusion in the formed part were studied by OM and EDS, moreover, the content of residual austenite was measured by XRD. The results indicated that the cracks were liquid hot cracks. In course of forming with multi-layers and multi-paths, the segregation comprised of Mn and Si oxidate, Mo carbide and Ni intermetallic compound were the internal cause for the cracks formation, while the tension stress was the external cause. By properly matching the contents of Mn, Ni and Si elements, purifying the weld metal with rear earth elements cerium, adopting the orthogonal deposi-

tion paths layer by layer and prolonging the interfomational intervals, the cracks could be avoided.

Key words: surfacing; rapid forming; metal cored wires; cracks; segregation

Effect of loading rate on shear strength of SnAgCu solder joint LU Wei, ZHANG Ning, SHI Yaowu, LEI Yongping (School of Materials Science and Engineering, Beijing University of Technology, Beijing 100124, China). p. 57—60

Abstract: Effect of loading rate on shear strength and fracture mode of SnAgCu (SAC) lead-free solder joint was investigated. The Ag content of the solders used in the experiment was 1% to 3%. The loading rate of the solder joint was 0.01 mm/s to 10 mm/s. The results indicated that the shear strength increased with the increase of loading rate and fracture with ductile feature occured inside the solder when the loading rate was less than 1 mm/s. When loading rate reached to 10 mm/s, the shear strength decreased and brittle fracture occured in the intermetallic compounds layer of joint. Moreover, shear strength increased with Ag content of solder increased at low loading rate, while the shear strength of solder joint with 2% Ag was the lowest at high loading rate.

Key words: lead-free solder; loading rate; shear strength

Effect of vanadium on property of Fe-Cr-C hardfacing alloy WANG Zhihui, HE Dingyong, YU Changli, JIANG Jianmin (College of Materials Science and Engineering, Beijing University of Technology, Beijing 100124, China). p. 61—64

Abstract: Vanadium was added to Fe-Cr-C hardfacing alloy and its effect on the property of the alloy when welded and reheated was studied. The hardfacing layers were produced on Q235 mild steel by submerged arc welding method. The microstructures, worn surface of the overlayer were examined by means of optical microscope and scanning electron microscopy (SEM). Abrasive wear resistance and hardness were tested. The results showd that heating process had effect on the hardness of the alloy. The hardness of matrix decreased more than 22% by reheating. The max hardness decreased 37.7% with no vanadium. But it has little effect on the hardness of primary carbide of which the hardness decreased only 1.4%-11.3% by reheating. Vanadium could increase the abrasion property of post-heated Fe-Cr-C hardfacing alloy. Using the loss weight of quenched 45# sample as abrasion test bench mark, the lative abrasion value of the alloy content of 0.4% vanadium was 1.9. In the same condition, that of the alloy with no vanadium content was only 1.3. The abrasion property increased 46%.

Key words: Fe-Cr-C hardfacing alloy; vanadium element; post heat treatment; carbide; abrasion wear

Simulation of temperature field and residual stress field of thin inner layer on butt welding of clad pipe YU Jianrong, HE Xiaoxiang[2], WU Bo, CHEN Haiyang, LI Xiaodong (1. School of Mechanical Engineering, Beijing Institute of Petrochemical Technology, Beijing 102617, China; 2. College of Mechanical and Electrical Engineering, Beijing University of Chemical Technology, Beijing 100029, China). p. 65—68

Abstract: The clad pipe has a thin inner layer made of stainless steel and a thick outer layer made of carbon steel, and the outer layer has some restriction on the temperature change surrounding the inner layer when butt-welding the inner layer. With finite element method, the temperature field was computed when butt-welding inner layer and the stress field of inner layer was computed after butt welding. The convection, radiation and contact effect between the two layers were considered in the FEM model as well as temperature depended material properties. Internal heat generation loading method was applied to simulate heat source, and model change ability to simulate butt-weld. The velocity of inner layer butt-weld, the temperature and stress field of the inner layer were discussed. Meanwhile the influence of the properties of material, geometry of the plate and the welding heat input on buckling distortion were analyzed based on the simulations. The results indicate that the geometry of the plate and the welding heat input have more effect on distortion than the properties of material.

Key words: clad pipe; butt-weld; finite element analysis; stress field; contact effect

Microstructure characteristic and performance of bonding interface between titanium alloy/copper/GCr15 LIU Shuying, ZHANG Guifeng, LU Guangbao, XU Peili, WANG Yawei (1. Henan Province Key Laboratory of Advanced Non-ferrous Metals, School of Materials Science and Engineering, Henan University of Science and Technology, Luoyang 471003, Henan, China; 2. Welding Research Institute, Xi'an Jiaotong University, Xi'an 710049, China; 3. Department of Electrical and Electronic, Henan Technician College of Economics and Business, Xinxiang 453700, Henan, China; 4. Shanghai Heavy Machinery Plant Limited Corporation, Shanghai 200245, China). p. 69—72, 76

Abstract: Difficulty for diffusion bonding of different structure of titanium alloy/bearing steel restricts the application of titanium alloy. The mechanical properties of Ti-6Al-4V/Cu/GCr15 joints were evaluated by electronic tensile machine. The microstructure characteristic and performance of the bonding interface were analyzed by scanning electron microscopy and EDX. Microhardness, the fracture characteristics and area of intermetallic compounds of the joints were analyzed by X-ray diffraction. The results indicated that the tensile strength of the joints under the bonding time 1.8 ks, pressure 4.9 MPa, rises with the bonding temperature, the tensile strength of joint reaches a maximum of 206 MPa in 1 273 K. The extension bonding time caused the intermetallic compound thickness to increase which would do harm to the joints performance. α-Ti(Cu) solid solution which was generated in bonding interface was advantageous to enhance the joints performance. However, the Ti_xCu_y had more influence on joints performance which was Ti_2Cu, Ti_2Cu_3, (Ti_3Cu_4) FeTi, those caused the joint strength to go down. Copper foil should not be too thick to be as interlayer in titanium/GCr15.

Key words: interlayer; diffusion bonding; bonding interface; tensile strength; intermetallic compounds

Heat source modeling and power density analysis for vacuum electron beam welding LUO Yi[2], XU Huibin, LI Chuntian, WU Guangfeng (1. School of Material Science and Engineering, Chongqing University of Technology, Chongqing 400050, China; 2. School of Material Science and Engineering, Northwestern Polytechnical University, Xi'an 710072, China). p. 73—76